Research Article

GC-MS Analysis and Inhibitory Evaluation of *Terminalia catappa* Leaf Extracts on Major Enzymes Linked to Diabetes

Franklyn Nonso Iheagwam ![ORCID],[1,2] **Emmanuel Nsedu Israel,**[1] **Kazeem Oyindamola Kayode,**[1] **Opeyemi Christianah De Campos,**[1,2] **Olubanke Olujoke Ogunlana,**[1,2] **and Shalom Nwodo Chinedu**[1,2]

[1]*Department of Biochemistry, Covenant University, Canaanland, P.M.B. 1023 Ota, Ogun State, Nigeria*
[2]*Covenant University Public Health and Wellbeing Research Cluster (CUPHWERC), Covenant University, Canaanland, P.M.B. 1023 Ota, Ogun State, Nigeria*

Correspondence should be addressed to Franklyn Nonso Iheagwam; franklyn.iheagwam@covenantuniversity.edu.ng

Terminalia catappa leaves are used in managing both diabetes mellitus and its complications in Southwest Nigeria. However, its inhibitory activity on enzymes implicated in diabetes is not very clear. This study investigated the *in vitro* inhibitory properties and mode of inhibition of *T. catappa* leaf extracts on enzymes associated with diabetes. The study also identified some bioactive compounds as well as their molecular interaction in the binding pocket of these enzymes. Standard enzyme inhibition and kinetics assays were performed to determine the inhibitory effects of aqueous extract (TCA) and ethanol extract (TCE) of *T. catappa* leaves on α-glucosidase and α-amylase activities. The phytoconstituents of TCA and TCE were determined using GC-MS. Molecular docking of the phytocompounds was performed using Autodock Vina. TCA and TCE were the most potent inhibitors of α-glucosidase ($IC_{50} = 3.28 \pm 0.47$ mg/mL) and α-amylase ($IC_{50} = 0.24 \pm 0.08$ mg/mL), respectively. Both extracts displayed a mixed mode of inhibition on α-amylase activity, while mixed and noncompetitive modes of inhibition were demonstrated by TCA and TCE, respectively, on α-glucosidase activity. The GC-MS analytic chromatogram revealed the presence of 24 and 22 compounds in TCE and TCA, respectively, which were identified mainly as phenolic compounds, terpenes/terpenoids, fatty acids, and other phytochemicals. The selected compounds exhibited favourable interactions with the enzymes compared with acarbose. Overall, the inhibitory effect of *T. catappa* on α-amylase and α-glucosidase may be ascribed to the synergistic action of its rich phenolic and terpene composition giving credence to the hypoglycaemic nature of *T. catappa* leaves.

1. Introduction

Diabetes mellitus (DM) is an endocrine, chronic, noncommunicable disease plaguing the world populace with a rapid increase. A reported 425 million individuals were globally affected by DM, while 629 million people have been projected to be affected by 2045 [1]. DM is characterized by hyperglycaemia as a consequence of impaired insulin secretion (as experienced in type 1 diabetes) or insulin resistance (as experienced in type 2 diabetes) resulting in diabetic complications such as diabetic retinopathy, neuropathy, and nephropathy [2]. Type 2 diabetes (T2D) is the most prevalent type of DM affecting over 90% of people diagnosed with this disease [3]. Lifestyle modification through exercise and diet as well as oral medications such as metformin, pioglitazone, and acarbose to decrease hepatic glucose output and insulin sensitivity improvement and reduce starch digestibility, respectively, are management methods currently employed in T2D [4].

Terminalia catappa Linn, commonly known as Indian almond, belongs to the Combretaceae family and grows in the tropics of Asia, Africa, and Australia [5]. In urban regions where these trees are found, the leaves form a menace and are the major constituents of generated lignocellulosic waste. In Southwest Nigeria, it is commonly called "igi furutu" or "igifuruntu," and various plant parts are used to treat diabetic complications by the locals [6]. Several studies have reported different activities of *T. catappa* extracts such as hepatoprotective effects, anticancer property, antimutagenic activity, and antiaging property [7]. Divya and Anand [8] have also reported on the inhibitory property of *T. catappa* methanolic leaf extract on diabetic-linked enzymes. Despite this antidiabetic claim by the locals, the elaborate antidiabetic mechanism is far from clear. This study assessed the inhibitory properties of *T. catappa* leaf extracts on α-glucosidase and α-amylase, the mode of enzyme inhibition, as well as identified phytocompounds present and proposed the molecular mechanism of binding in the active sites of the enzymes.

2. Materials and Methods

2.1. Materials. α-Glucosidase, α-amylase enzymes, and their substrates were acquired from Solarbio Life Sciences, Beijing, China. Other chemicals were products of Sigma-Aldrich, St. Louis, USA.

2.2. Plant Collection, Identification, and Extraction. Mature *T. catappa* leaves were sourced between October and December 2016, from Covenant University compound. They were identified by Dr. J. O. Popoola of Biological Sciences Department and voucher specimen deposited at Biological Sciences Department herbarium, Covenant University, Ota, Ogun State, with herbarium number TC/CUBio/H809. Aqueous *T. catappa* (TCA) and ethanol *T. catappa* (TCE) leaf extracts were prepared as reported by Iheagwam et al. [9]. The leaves were cut, air-dried, pulverised, and macerated in distilled water and ethanol (80%), respectively, at 1 : 10 (w/ v) ratio for 72 hrs. The obtained filtrates were concentrated using a rotary evaporator.

2.3. Antidiabetic Assessment

2.3.1. α-Glucosidase Inhibitory Activity. α-Glucosidase inhibitory activity of the extracts was evaluated according to the method described by Ibrahim and Islam [10] with slight modification. Various extract concentration and acarbose (1–5 mg/mL, 250 μL) were incubated at 37°C for 15 min with α-glucosidase solution (1 U/mL, 500 μL). ρ-Nitrophenyl-α-D-glucopyranoside (pNPG) solution (5 mM, 250 μL) was thereafter added, and the resulting mixture was incubated for 20 min at 37°C. The reaction was terminated by adding Na_2CO_3 (0.2 M, 100 μL), and absorbance was measured at 405 nm. Phosphate buffer (100 mM) was used as control in place of inhibitors. Inhibitory activity was calculated using the following equation:

$$\% \text{ inhibition } = 100 \times \left(\frac{A_c - A_s}{A_c} \right), \tag{1}$$

where A_s = absorbance in the presence of sample and A_c = absorbance of control. All solutions were prepared in 0.1 M phosphate buffer (pH 6.8).

The method of Sabiu and Ashafa [11] was adopted for α-glucosidase inhibitory kinetics. Extract (5 mg/mL, 250 μL) was preincubated with α-glucosidase solution (1 U/mL, 500 μL) for 10 min at 25°C. Varying pNPG concentrations (0.15–5 mg/mL, 250 μL) were added and incubated for 10 min at 25°C to both sets of reaction mixtures to start the reaction. Thereafter, Na_2CO_3 (0.2 M, 500 μL) was added to stop the reaction. For the control kinetic reaction, 100 mM phosphate buffer (pH 6.8, 250 μL) was used in place of the extract. Reaction rates (v) were calculated, and double reciprocal plots of α-glucosidase inhibition kinetics were determined.

2.3.2. α-Amylase Inhibitory Activity. α-Amylase inhibitory activity of the extracts was evaluated by adopting the method described by Ibrahim and Islam [10] with slight modification. Various extract concentrations (1–5 mg/mL, 250 μL) and acarbose were incubated at 37°C for 20 min with amylase solution (2 U/mL, 500 μL). Starch solution (1%, 250 μL) was later added to the reaction mixture and incubated at 37°C for 1 h. Dinitrosalicylic acid (DNS) colour reagent (1 mL) was added to stop the reaction. The resulting mixture was boiled for 10 min, and absorbance was measured at 540 nm. Phosphate buffer (100 mM) was used as control in place of inhibitors. The α-amylase inhibitory activity was calculated using the following formula:

$$\% \text{ inhibition } = 100 \times \left(\frac{A_c - A_s}{A_c} \right), \tag{2}$$

where A_s = absorbance in the presence of sample and A_c = absorbance of control. All solutions were prepared in 100 mM phosphate buffer (pH 6.8).

The method of Sabiu and Ashafa [11] was adopted for α-amylase inhibitory kinetics. In brief, extract (250 μL, 5 mg/ mL) was incubated with α-amylase (2 U/mL, 500 μL) for 10 min, before the addition of various substrate concentrations (0.3–10 mg/mL, 250 μL). The reaction proceeded as highlighted for α-glucosidase. α-Amylase inhibition kinetics was determined from the Lineweaver–Burk double reciprocal plot.

2.4. Gas Chromatography-Mass Spectroscopy (GC-MS) Analysis. The GC-MS analysis of *T. catappa* extracts was carried out using GCMS-QP2010SE SHIMADZU, Japan, fused with the Optima 5 ms capillary column (30 × 0.25 mm) of 0.25 μm film thickness following the described method of Ajiboye et al. [12] with slight modifications. The gas chromatography conditions were as follows: pure helium carrier gas (flow rate: 1.56 mL/min; linear velocity: 37 cm/s), initial column oven temperature (60°C) programmed to increase to 160°C at the rate of 10°C/min and then finally to 250°C with a

hold time of 2 min/increment, and an injection volume of $0.5\,\mu$L in the splitless mode with a split ratio of 1 : 1 and injector temperature set at 200°C. Mass spectrophotometer conditions were as follows: ion source temperature (230°C), interface temperature (250°C), solvent delay at 4.5 min, and acquisition in a scan range of 50–700 amu. Electron ionization mode and multiplier voltage were set at 70 eV and 1859 V, respectively. Retention time, fragmentation pattern, and mass spectral data of the unknown components in the extracts were compared with those in Wiley and National Institute of Standards and Technology (NIST) libraries for compound identification.

2.5. In Silico α-Glucosidase and α-Amylase Inhibition Prediction

2.5.1. Ligand and Protein Modelling. The structures of the GC-MS identified compounds with ≥5% abundance were prepared as reported by Iheagwam et al. [13]. The 3D structure of α-glucosidase and α-amylase was modelled using the crystal structures with PDB codes 5kzw and 1b2y, respectively, obtained from RCSB protein data bank as templates in SWISS-MODEL [14].

2.5.2. Virtual Screening, Drug-Likeness, and Molecular Docking. Virtual screening of selected identified ligands, analysis of drug-likeness using the rule of five (RO5), and molecular docking were carried out according to the methodology of Iheagwam et al. [13]. However, grid dimensions of the binding pockets were $60 \times 40 \times 32$ and $40 \times 34 \times 40$ points separated by 1 Å for α-glucosidase and α-amylase, respectively. Inhibition constant (K_i) of docked ligands were calculated by using the following formula:

$$K_i = 10^{[\text{binding energy (BE)}/1.366]}. \qquad (3)$$

2.6. Statistical Analysis. Data were analysed using SPSS version 25 (IBM Corp., New York, USA) and subjected to one-way analysis of variance (ANOVA) using the Duncan multiple range post hoc test. Values were reported as mean ± standard deviation (SD) of three (3) replicates and considered significantly different at $p < 0.05$.

3. Results

For the α-glucosidase inhibitory activity of TCA and TCE as shown in Figure 1, a significantly ($p < 0.05$) lower inhibition by the extracts was observed at all concentrations relative to control. TCA exhibited a significantly ($p < 0.05$) higher inhibition of α-glucosidase activity compared to TCE. Nonetheless, at lower concentrations (1–3 mg/mL), there was no difference between the inhibitory activities of TCA and TCE. These were further supported by a lower IC_{50} value (2.23 ± 0.21 mg/mL) for acarbose when compared with TCA (3.28 ± 0.47 mg/mL) and TCE (3.78 ± 0.26 mg/mL (Table 1). The kinetic study on the inhibition mode using the double reciprocal plot revealed TCE exhibited a noncompetitive

mode of inhibition with a common K_m value of 0.19 mM and V_{max} value of 0.13 mM/min, while TCA exhibited a mixed mode of inhibition with a K_m value of 0.77 mM and V_{max} value of 0.1 mM/min (Figure 2).

The percentage inhibition of α-amylase activity by *T. catappa* leaf extracts is presented in Figure 3. Though a concentration-dependent effect was observed, TCE inhibitory activity was significantly ($p < 0.05$) higher than TCA and acarbose at all concentrations. TCA elicited inhibitory effects that competed favourably with the standard drug (acarbose). These results were supported with an IC_{50} of 0.24 ± 0.08, 0.75 ± 0.14, and 0.85 ± 0.18 mg/mL recorded for TCE, TCA, and acarbose, respectively (Table 1). TC extracts displayed a mixed mode of inhibition on α-amylase activity with a V_{max} value of 0.013 and 0.016 mM/min and K_m values of 2.27 and 2.22 mg for TCE and TCA, respectively (Figure 4), from the Lineweaver–Burk double reciprocal plot.

The GC-MS chromatogram as shown in Figures 5 and 6 confirmed the presence of various phytochemicals with different retention times for TCE and TCA, respectively. A total of 27 and 29 peaks were identified in TCE and TCA chromatograms, respectively.

The identified phytochemicals present in TCE and TCA are shown in Tables 2 and 3, respectively, based on their retention time, abundance, and compound classification. GC-MS analysis revealed the presence of 24 compounds in TCE and 22 compounds in TCA. Seven compounds were found in both extracts; however, phytol and *n*-hexadecanoic acid were higher in TCE, while 4H-pyran-4-one, 2,3-dihydro-3,5-dihydroxy-6-methyl-, benzofuran, 2,3-dihydro-, 2-methoxy-4-vinylphenol, and 9,12-octadecadienoic acid (Z,Z)- were higher in TCE. It was also observed that there was no much difference in the abundance of vitamin E in both extracts.

For TCE, 9, 26, 13, 30, and 25% of the identified compounds were classified as carbohydrates, fatty acids, hydrocarbons, phenolics, and terpenes/terpenoids, respectively (Table 2), while for TCA, 5, 5, 33, 33, 19, and 5% of the identified compounds were classified as alcohols, alkaloids, fatty acids, phenolics, terpenes/terpenoids, and pyrethrin, respectively (Table 3).

From the GC-MS analyses as shown in Tables 2 and 3, 12 identified compounds were found to have an abundance of 5% or more. They ranged from [1,1′-bicyclopropyl]-2-octanoic acid, 2′-hexyl-, methyl ester (5.2%), to phytol (29.54%). Virtual screening results revealed these compounds had relatively lower binding energy than acarbose (−126.81) when docked in the binding site of α-amylase. However, only vitamin E (−82.91) and ethyl-α-D-glucopyranoside (−78.11) were relatively comparable with the standard (Table 4).

As illustrated in Table 5, the same observation was also made after screening the compounds in the binding site of α-glucosidase. Besides ethyl-α-D-glucopyranoside (−79.92) and vitamin E (−89.64), *n*-hexadecanoic acid (−81.89) and phytol (−80.87) binding affinities were also comparable with acarbose (−115.55).

When the hit compounds were screened for their drug-likeness, they all obeyed Lipinski's RO5. However, phytol
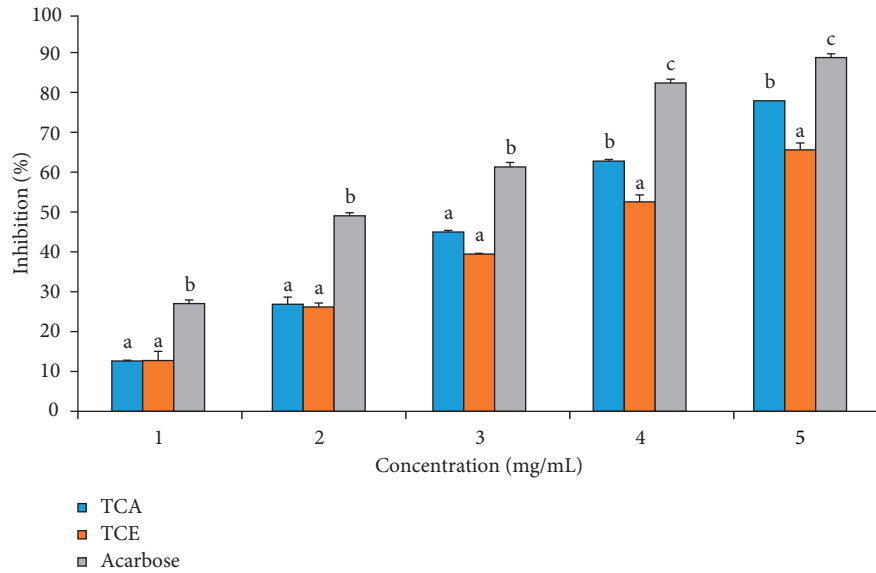
FIGURE 1: *T. catappa* leaf extract inhibitory effect on α-glucosidase activity. Bars are expressed as means ± SD of triplicate determinations. Bars with different superscripts on each concentration denote significant difference ($p < 0.05$).

TABLE 1: IC$_{50}$, V_{max}, and K_m values of *T. catappa* leaf extracts on α-glucosidase and α-amylase.

	α-Glucosidase			α-Amylase		
	IC$_{50}$ (mg/mL)	V_{max} (mM/min)	K_m (mM)	IC$_{50}$ (mg/mL)	V_{max} (mM/min)	K_m (mg)
TCE	3.78 ± 0.26^c	0.13	0.19	0.24 ± 0.08^a	0.013	2.27
TCA	3.28 ± 0.47^b	0.10	0.77	0.75 ± 0.14^b	0.016	2.22
Acarbose	2.23 ± 0.21^a	—	—	0.85 ± 0.18^b	—	—
Control	—	0.35	0.19	—	0.025	0.43

Data are represented as mean ± SD ($n = 3$). Values with different superscripts down a column are significantly different at $p < 0.05$. IC$_{50}$: half maximal inhibitory concentration; V_{max}: maximum velocity; K_m: Michaelis constant.
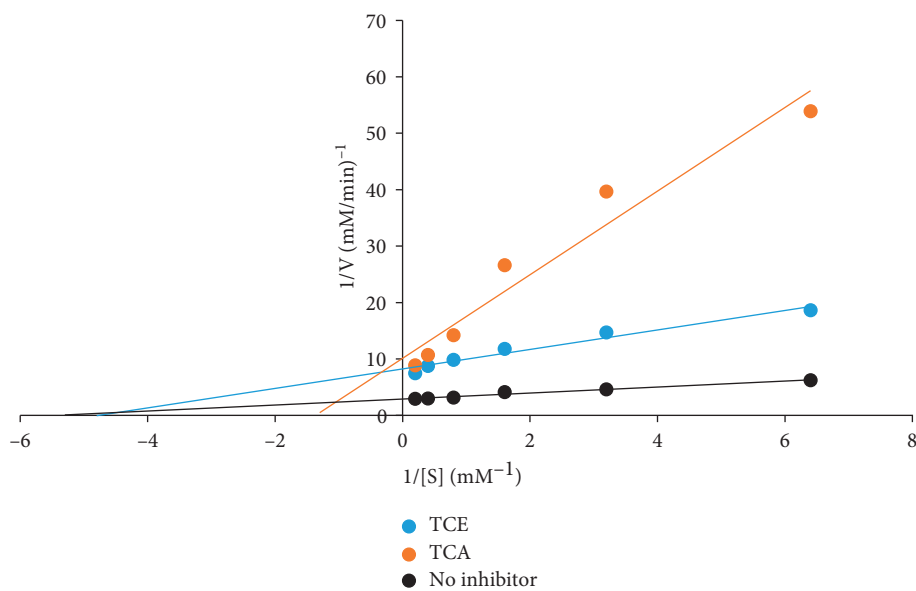

FIGURE 2: *T. catappa* leaf extract mode of inhibition on α-glucosidase activity.
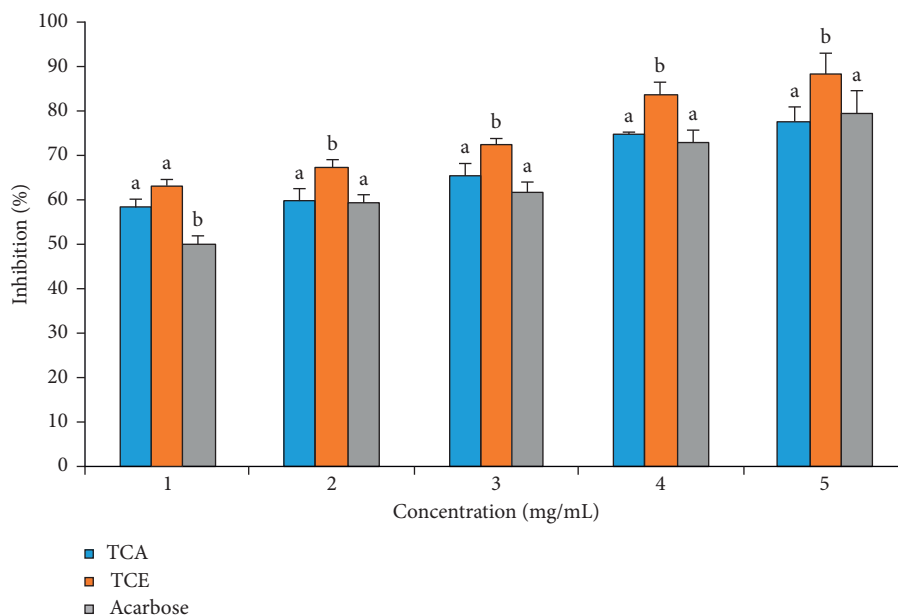
Figure 3: *T. catappa* leaf extract inhibitory effect on α-amylase activity. Bars are expressed as means ± SD of triplicate determinations. Bars with different superscripts on each concentration denote significant difference ($p < 0.05$).
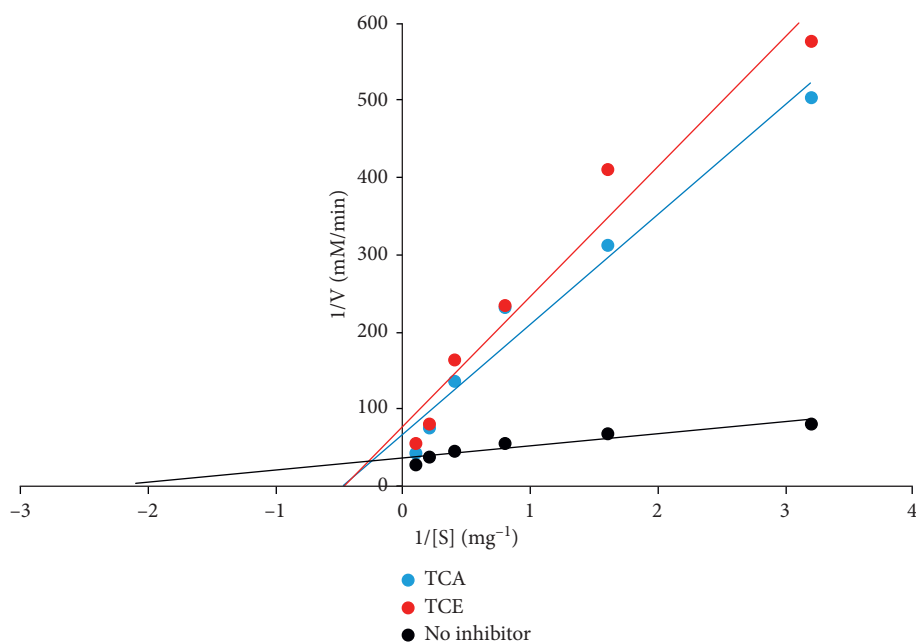

Figure 4: *T. catappa* leaf extract mode of inhibition on α-amylase activity.

and vitamin E, on the one hand, violated only the octanol-water partition coefficient due to higher values than the RO5 threshold as presented in Table 6. Acarbose, on the other hand, violated 3 variants.

The binding affinity of the selected compounds as shown in Table 7 using Autodock Vina ranged from −6.0 to 8.0 kcal/mol and −5.1 to 5.9 kcal/mol for α-amylase and α-glucosidase, respectively. These values though lower were comparable with acarbose where −8.3 was recorded for α-amylase and −7.4 for α-glucosidase. Concomitantly, 1.39

to 40.51 μM was the α-amylase inhibition constant (K_i) recorded for the compounds compared to 0.84 μM for acarbose, while 47.95 to 184.70 μM was the α-glucosidase K_i recorded for the compounds compared to 3.83 μM for acarbose.

As depicted in Figure 7, the ligands bound to both the active and allosteric sites of the enzymes. It further justified the *in vitro* results as the majority of the ligands favoured active site binding compared to the allosteric site. Hydrogen, van der Waals, and π bonds were the
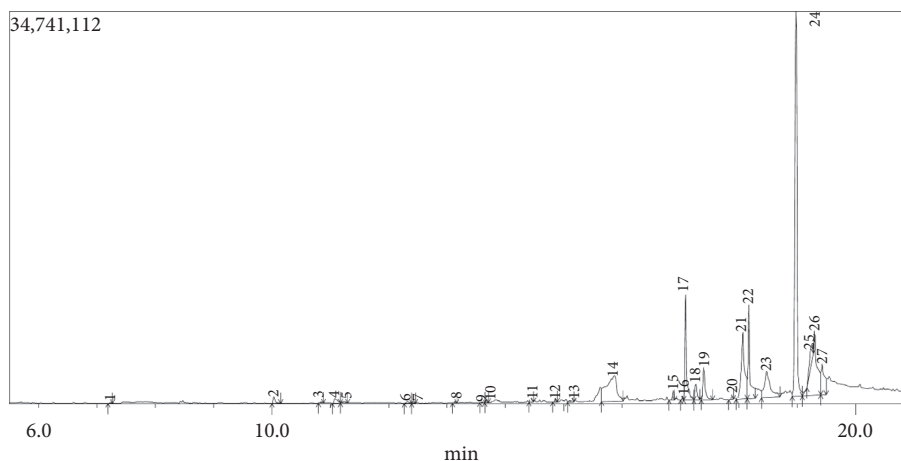
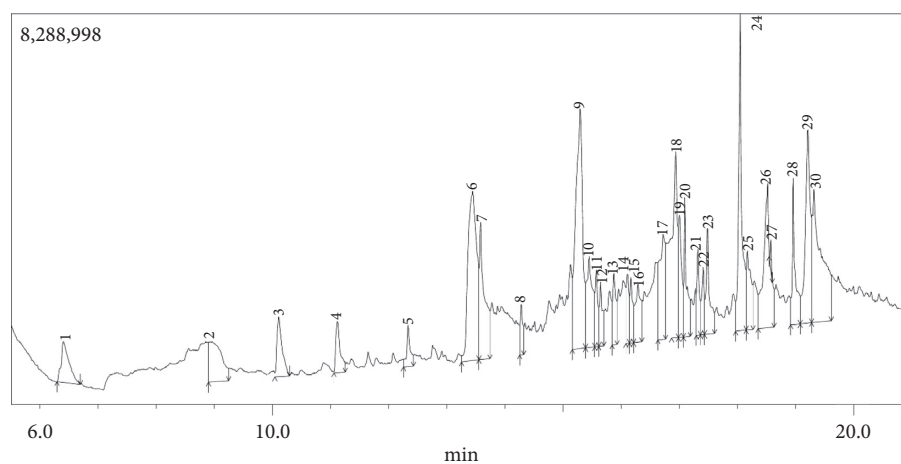Figure 5: GC chromatogram of *T. catappa* ethanolic leaf extract.

Figure 6: GC chromatogram of *T. catappa* aqueous leaf extract.

common interactions displayed between the compounds and amino acids present in the binding sites of the enzymes. Trp 73, Trp 74, Tyr 77, Tyr 166, and Ile 250 were common amino acids stabilising the binding of vitamin E and acarbose in the binding pocket of α-amylase, while in the α-glucosidase binding pocket, Ala 284, Asp 616, and Trp 481 were common amino acids stabilising phytol, vitamin E, and acarbose (Figures 8 and 9).

4. Discussion

α-Glucosidase and α-amylase are major enzymes that metabolise carbohydrate in the digestive tract thereby affecting carbohydrate metabolism. Drugs which illicit their pharmacological action by inhibiting these enzymes are used as therapeutic control in managing diabetes through the control of postprandial hyperglycaemia [15, 16]. Research on inhibitors of these enzymes especially from medicinal plants has been intensified due to their claim of being inexpensive and less toxic compared to synthetically derived medications such as acarbose and

miglitol with similar mechanisms of action [17]. Promising inhibitory activity of *T. catappa* leaf extracts was exhibited on α-glucosidase and α-amylase as previously reported in a dose-dependent manner [8]. Nonetheless, this potential was more portrayed in α-amylase activity as *T. catappa* leaf extracts exhibited a better inhibitory potential than acarbose. This was corroborated by various studies that have previously reported a higher inhibitory potential of medicinal plant extracts than acarbose [16, 18, 19]. It was also noteworthy that our extracts had better α-glucosidase and α-amylase inhibitory activities than those reported for *Nicotiana tabacum* and *Calotropis procera* leaf extracts [20, 21]. The reported α-glucosidase and α-amylase inhibitory activities of *Sutherlandia montana* and *Aerva lanata* (ethanol) leaf extracts were higher than our extracts except for *A. lanata* aqueous leaf extract α-amylase inhibitory activity which was reported to be lower than ours [4, 22]. Contrary to the reports of Xu et al. [23] and Wan et al. [24], the inhibitory activity of *T. catappa* leaf extracts was higher on α-amylase than on α-glucosidase at the varied

TABLE 2: GC-MS identified phytochemicals present in *T. catappa* ethanolic leaf extract.

Peak no.	Compound name	Retention time (min)	Area (%)	Molecular weight (g/mol)	Formula	Classification of compound
1	2-Furancarboxaldehyde, 5-methyl-	7.227	0.05	110.11	$C_6H_6O_2$	Carbohydrate
2	4H-Pyran-4-one, 2,3-dihydro-3,5-dihydroxy-6-methyl-	10.034	0.54	144.12	$C_6H_8O_4$	Phenolics
3	2,5-Dimethyl-1-hepten-4-ol	10.839	0.1	142.24	$C_9H_{18}O$	Terpene
4	Benzofuran, 2,3-dihydro-	11.084	0.61	120.15	C_8H_8O	Phenolics
5	Cyclopentanol, 1-(1-methylene-2-propenyl)-	11.235	0.24	138.21	$C_9H_{14}O$	Terpene
6	2-Methoxy-4-vinylphenol	12.326	0.2	150.17	$C_9H_{10}O_2$	Phenolics
7	7-Oxabicyclo[4.1.0]heptane, 1,5-dimethyl-	12.417	0.08	126.20	$C_8H_{14}O$	Phenolics
8	1-Tetradecanol	13.133	0.09	214.39	$C_{14}H_{30}O$	Fatty acid
9	cis-Z-α-Bisabolene epoxide	13.6	0.07	220.35	$C_{15}H_{24}O$	Terpenoid
10	2-(3,3-Dimethyl-but-1-ynyl)-1,1-dimethyl-3-methylene-cyclopropane	13.673	0.1	162.27	$C_{12}H_{18}$	Hydrocarbon
11	Phenol, 2,6-bis(1,1-dimethylethyl)-	14.429	0.35	206.32	$C_{14}H_{22}O$	Phenolics
12	2(4H)-Benzofuranone, 5,6,7,7a-tetrahydro-4,4,7a-trimethyl-, (R)-	14.851	0.15	180.24	$C_{11}H_{16}O_2$	Phenolics
13	10-Heneicosene (c,t)	15.143	0.33	294.60	$C_{21}H_{42}$	Hydrocarbon
14	Ethyl-α-D-glucopyranoside	15.863	10.38	208.21	$C_8H_{16}O_8$	Carbohydrate
15	6-Methyl-cyclodec-5-enol	16.876	0.59	168.28	$C_{11}H_{20}O$	Phenolics
16, 17	Phytol, acetate	17.09	6.92	338.60	$C_{22}H_{42}O_2$	Terpenoid
20	9-Octadecene, 1-methoxy-, (E)-	17.88	0.25	282.50	$C_{19}H_{38}O$	Hydrocarbon
21	n-Hexadecanoic acid	18.072	8.95	256.43	$C_{16}H_{32}O_2$	Fatty acid
22	Hexadecanoic acid, ethyl ester	18.172	6.83	284.50	$C_{18}H_{36}O_2$	Fatty acid ethyl ester
23	Vitamin E	18.478	6.25	430.70	$C_{29}H_{50}O_2$	Terpenoid
18, 19, 24	Phytol	18.985	29.54	296.50	$C_{20}H_{40}O$	Phytosterol
25	9,12-Octadecadienoic acid (Z,Z)-	19.257	2.46	280.40	$C_{18}H_{32}O_2$	Fatty acid
26	Oleic acid	19.293	17.1	282.50	$C_{18}H_{34}O_2$	Fatty acid
27	4-Decenoic acid, ethyl ester, (Z)-	19.425	3.79	198.30	$C_{12}H_{22}O_2$	Fatty acid ethyl ester

TABLE 3: GC-MS identified phytochemicals present in *T. catappa* aqueous leaf extract.

Peak no.	Compound	Retention time (min)	Area (%)	Molecular weight (g/mol)	Formula	Classification of compound
1	2,3-Butanediol	6.399	2.14	90.12	$C_4H_{10}O_2$	Alcohol
2	Diglycerol	8.958	3.31	166.17	$C_6H_{14}O_5$	Fatty acid
3	4H-Pyran-4-one, 2,3-dihydro-3,5-dihydroxy-6-methyl-	10.105	2.03	144.12	$C_6H_8O_4$	Phenolics
4	Benzofuran, 2,3-dihydro-	11.115	1.49	120.15	C_8H_8O	Phenolics
5	2-Methoxy-4-vinylphenol	12.334	0.98	150.17	$C_9H_{10}O_2$	Phenolics
6	1,2,3-Benzenetriol	13.444	9.63	126.11	$C_6H_6O_3$	Phenolics
7	1,2,4-Benzenetriol	13.58	4.65	126.11	$C_6H_6O_3$	Phenolics
8	2-Cyclohexen-1-one, 3-(hydroxymethyl)-6-(1-methylethyl)-	14.279	0.92	168.23	$C_{10}H_{16}O_2$	Terpenoid
9	9-Oxabicyclo[3.3.1]nonane-2,6-diol	15.295	11.02	158.19	$C_8H_{14}O_3$	Phenolics
10, 25	9,9-Dimethoxybicyclo[3.3.1]nona-2,4-dione	15.448	3.36	212.24	$C_{11}H_{16}O_4$	Phenolics
13, 15	9,10-Secocholesta-5,7,10(19)-triene-1,3-diol, 25-[(trimethylsilyl)oxy]-, (3β,5Z,7E)-	15.873	1.61	212.24	$C_{30}H_{52}O_3Si$	Terpenoid
14	8-Methyl-6-nonenoic acid	16.111	1.12	170.25	$C_{10}H_{18}O_2$	Fatty acid
11, 12, 16–19	[1,1′-Bicyclopropyl]-2-octanoic acid, 2′-hexyl-, methyl ester	16.942	5.2	322.50	$C_{21}H_{38}O_2$	Fatty acid methyl ester
21	4-Decenoic acid, 3-methyl-, (E)-	17.322	1.39	184.27	$C_{11}H_{20}O_2$	Fatty acid
23	Cycloheptanone imine, 2,2,7,7-tetramethyl-	17.488	2.52			Alkaloid
24	n-Hexadecanoic acid	18.049	6.77	256.43	$C_{16}H_{32}O_2$	Fatty acid
26	Vitamin E	18.523	6.33	430.70	$C_{29}H_{50}O_2$	Terpenoid
27	Jasmolin II	18.572	0.15	374.50	$C_{22}H_{30}O_5$	Pyrethrin
20, 22, 28	Phytol	18.964	2.77	296.50	$C_{20}H_{40}O$	Phytosterol
29	9,12-Octadecadienoic acid (Z,Z)-	19.214	6.39	280.40	$C_{18}H_{32}O_2$	Fatty acid
30	17-Octadecynoic acid	19.318	8.31	167.29	$C_{11}H_{21}N$	Fatty acid

TABLE 4: Virtual screening results of identified ligand on α-amylase using iGEMDOCK.

S. no	Compound	(kcal/mol)			
		TE	VdW	Hbond	Elec
1	[1,1-Bicyclopropyl]-2-octanoicacid, 2-hexyl-, methyl ester-	−71.55	−71.55	0.00	0.00
2	1,2,3-Benzenetriol	−62.38	−47.42	−14.96	0.00
3	Ethyl-α-D-glucopyranoside	−78.11	−55.12	−22.99	0.00
4	Hexadecanoic acid, ethyl ester	−65.40	−60.40	−5.00	0.00
5	n-Hexadecanoic acid	−65.71	−45.93	−16.41	−3.37
6	Oleic acid	−71.75	−51.69	−16.66	−3.41
7	Phytol acetate	−67.32	−66.64	−0.68	0.00
8	Phytol	−64.40	−53.90	−10.50	0.00
9	Vitamin E	−82.91	−76.90	−6.01	0.00
10	9,12-Octadecadienoic acid (Z,Z)-	−68.67	−59.76	−7.33	−1.61
11	9-Oxabicyclo[3.3.1]nonane-2,6-diol	−62.20	−37.56	−24.64	0.00
12	17-Octadecynoic acid	−74.92	−66.04	−9.25	0.37
13	Acarbose	−126.81	−64.99	−61.83	0.00

TE: total energy; VdW: van der Waals bond; Hbond: hydrogen bond; Elec: electrostatic bond.

TABLE 5: Virtual screening results of identified ligand on α-glucosidase using iGEMDOCK.

S. no	Compound	(kcal/mol)			
		TE	VdW	Hbond	Elec
1	9,12-Octadecadienoic acid (Z,Z)-	−74.89	−72.86	0.00	−2.02
2	9-Oxabicyclo[3.3.1]nonane-2,6-diol	−65.03	−46.52	−18.51	0.00
3	17-Octadecynoic acid	−71.74	−69.29	−1.90	−0.56
4	[1,1-Bicyclopropyl]-2-octanoicacid, 2-hexyl, methyl ester	−66.96	−64.46	−2.50	0.00
5	1,2,3-Benzenetriol	−70.52	−46.14	−24.38	0.00
6	Ethyl-α-D-glucopyranoside	−79.92	−53.16	−26.76	0.00
7	Hexadecanoic acid, ethyl ester	−69.78	−60.29	−9.49	0.00
8	n-Hexadecanoic acid	−81.89	−70.45	−11.44	0.00
9	Oleic acid	−76.72	−62.87	−13.84	0.00
10	Phytol acetate	−70.23	−70.23	0.00	0.00
11	Phytol	−80.87	−72.93	−7.95	0.00
12	Vitamin E	−89.64	−89.64	0.00	0.00
13	Acarbose	−115.55	−78.78	−36.77	0.00

TE: total energy; VdW: van der Waals bond; Hbond: hydrogen bond; Elec: electrostatic bond.

TABLE 6: Drug-likeness violation of selected virtual screened hit compounds.

S. no	Compound	MW	Log P	HA	HD	# Lipinski violations
1	Ethyl-α-D-glucopyranoside	208.21	−2.18	6	4	—
2	n-Hexadecanoic acid	256.42	4.19	2	1	—
3	Phytol	296.53	5.25	1	1	1
4	Vitamin E	430.71	6.14	2	1	1
5	Acarbose	645.6	−6.94	19	14	3
6	Lipinski rule details	≤500	≤5	≤10	≤5	

MW: molecular weight; log P: octanol-water partition coefficient; HA: hydrogen acceptor; HD: hydrogen donor.

concentrations and may be attributed to the different mechanism of action on these enzymes. This was further buttressed by the kinetic studies, where the TC extracts exhibited a mixed mode of inhibition on α-amylase, while mixed and uncompetitive inhibition mechanisms were observed for TCA and TCE, respectively, on α-glucosidase. The mixed mechanisms exhibited by TCA and TCE may suggest the bioactives present in the extracts may bind in the active site of these enzymes thereby reducing

the affinity of the substrate [25, 26]. Binding of these phytochemicals in the allosteric site is also a possible mechanism of action which may lead to a conformational change of these enzymes leading to a reduction in substrate affinity for the active site concomitantly hampering enzyme catalysis [25, 26]. The results suggest these extracts may have more affinity for the enzyme (E) than the enzyme-substrate complex (ES). The noncompetitive inhibition by TCE would suggest the phytochemicals

TABLE 7: Molecular docking analysis showing binding affinity, inhibition constant, and interacting residues in the binding site of α-amylase and α-glucosidase.

Protein	Compound	BE (kcal/mol)	K_i (μM)	Hb-IR	VdWb-IR	πb-IR
α-Amylase	Ethyl-α-D-glucopyranoside	−6.0	40.51	Arg 361, Arg 282, Asp 332, Ile 327, Gln 317, Gly 319	Leu 328, Trp 331, Thr 329, Asn 316, Arg 318, Phe 363, Ala 325	—
	Vitamin E	−8.0	1.39	—	Gln 78, Trp 74, Asp 315, Val 249, Glu 248, His 320	Val 178, Leu 180, Leu 177, His 314, Trp 73, Tyr 77, Tyr 166, Ile 250, Ala 213
	Acarbose	−8.3	0.84	Gly 321, His 320, Asp 212, Arg 210, Glu 248, Lys 215	His 216, Asp 315, Asp 251, His 314, Gln 78, Trp 73, Trp 74, Tyr 77, Leu 180, His 116, Ala 213, Ala 322, Ile 250, Tyr 166, Glu 255	Leu 177, Val 178
Glucosidase	Ethyl-α-D-glucopyranoside	−5.1	184.70	Gln 743, His 742	Val 740, Val 763, Val 755, Thr 768, Thr 753, Gly 765, Pro 754, Leu 756, Gln 757	Trp 804
	n-Hexadecanoic acid	−5.2	156.05	Val 358	Leu 195, Leu 577, Leu 574, Leu 565, Gly 605, Ala 604, Ala 582, Tyr 609, Pro 194, Thr 578, Thr 491, Phe 490, Arg 585	Leu 496, Ile 581
	Phytol	−5.5	94.11	—	Asp 282, Asp 616, Asp 404, Asp 443, Arg 600, Ile 441, Leu 405, Leu 650, Ser 676	Phe 525, Phe 649, Trp 481, Trp 376, His 674, Ala 284, Met 519,
	Vitamin E	−5.9	47.95	—	Arg 281, Arg 500, Ala 284, Ser 523, Met 519, Phe 649, Asp 616	Trp 376, Trp 481, Leu 283, Phe 525, Asp 262
	Acarbose	−7.4	3.83	Asn 524, Asp 282, Asp 404, Asp 616, Asp 518, Arg 600, Ser 676, Trp 481	—	Ala 284

BE: binding energy; K_i: inhibition constant; Hb-IR: hydrogen bond interacting residues; VdWb-IR: van der Waals bond interacting residues; πb-IR: pi bond interacting residues.
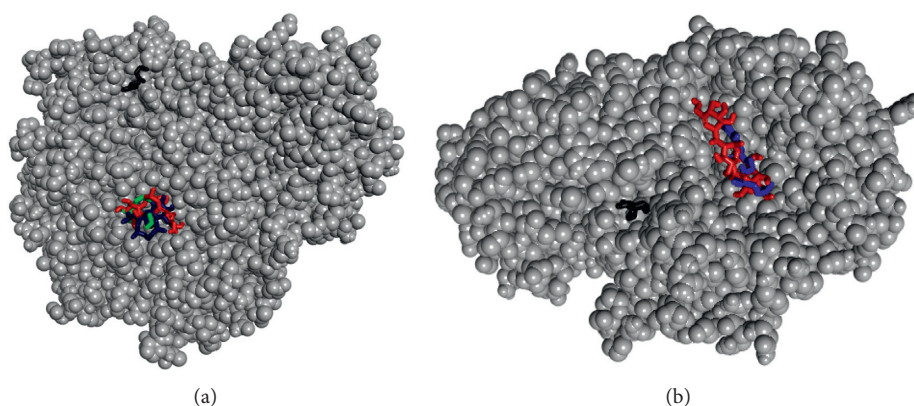

(a)   (b)

FIGURE 7: Binding of ligands in the active and allosteric pockets of (a) α-glucosidase and (b) α-amylase. The ligands ethyl-α-D-glucopyranoside, vitamin E, n-hexadecanoic acid, phytol, and acarbose were colour coded as black, blue, purple, green, and red, respectively.

present in the extract are noncompetitive and thus would bind to a site different from the α-glucosidase active site affecting catalysis without having an effect on substrate binding in the active site [27]. The observed inhibitory action observed for TC extracts may be attributed to the synergistic action of identified phytochemicals from the gas chromatogram. Fatty acids, phenolic compounds, and terpenes/terpenoids were the majority classes of identified phytochemicals in both extracts. Phenolic compounds and terpenoids have also been reported to elicit antioxidant properties and alleviate oxidative stress accumulation, in the process preventing the progression
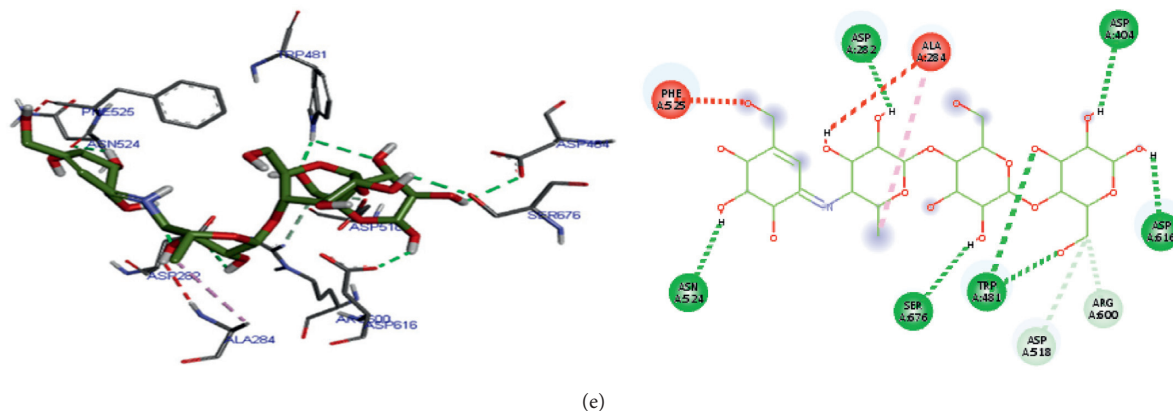
(a)

(b)

(c)

FIGURE 8: 3D and 2D diagram of (a) ethyl-α-D-glucopyranoside, (b) vitamin E, and (c) acarbose in their α-amylase binding pocket using Autodock Vina. Green and blue broken lines represent conventional and carbon-hydrogen bonds, respectively; magenta, purple, and orange represent π bonds, while red broken lines represent unfavourable bonds.

of diabetic complications [28]. Compounds such as phytol [29, 30], various terpenes and terpenoids [11], hexadecanoic acid, ethyl ester, and 9,12-octadecadienoic acid (Z,Z)- [31] have been reported to exhibit various antidiabetic activities. Furthermore, reports have it that hydrolysis of phenolic compounds leads to the

(a)

(b)

(c)

(d)

FIGURE 9: Continued.

(e)

FIGURE 9: 3D and 2D diagram of (a) ethyl-α-D-glucopyranoside, (b) *n*-hexadecanoic acid, (c) phytol, (d) vitamin E, and (e) acarbose in their α-glucosidase binding pocket using Autodock Vina. Green and blue broken lines represent conventional and carbon-hydrogen bonds, respectively, while magenta and red broken lines represent *p* and unfavourable bonds.

generation of shorter phenolic groups which accumulate, reduce oxidative stress, and inhibit amylase activity as well as other digestive enzymes reducing starch digestion [28, 32, 33]. This could also explain the better amylase inhibitory property of the extracts when compared with the glucosidase inhibitory activity. Pharmaceutical industries use structure-based drug design to solve challenges affecting integrated and classical drug design [34]. In lead compound development, compliance of test compound physicochemical properties (molecular mass, number of hydrogen bond donors and acceptors and so on) to Lipinski rule of 5 (RO5) is imperative to avoid failure during clinical trials [35, 36]. Compounds that pass RO5 (usually with none or one default) are predicted to have optimal pharmacokinetic properties, consequently subjecting them further to molecular docking [13]. Since all compounds passed RO5, they may exhibit good pharmacokinetic properties. Molecular docking further gave us a better understanding of the binding interaction between some identified phytochemicals and the key carbohydrate hydrolysing enzymes. The relatively lower binding affinity and inhibitory constant of the individual bioactives than acarbose could be due to the lesser number of hydrogen bonds present between the amino acids and the hydrogen donor/acceptor atoms in the ligands. This finding was contrary to what Pérez-Nájera et al. [37] reported on *Smilax aristolochiifolia* root extract and its compounds where the number of hydrogen bonds did not affect binding affinity. Vitamin E had the lowest free energy and K_i in amylase and glucosidase binding pockets which was comparable to acarbose. Consequently, it exhibited a more stable affinity with only a small concentration required to inhibit these enzymes [38]. Molecular docking further affirmed the *in vitro* inhibitory mechanisms as more identified compounds bound to the active site than the allosteric site signifying a preference for the (E) to elicit their potential pharmacological action [39]. The common interaction between Trp, Tyr, Ile, Ala, and Asp in the binding pockets of the enzymes and ligands (acarbose, vitamin E, and phytol) suggests nonpolar bonds (van der Waals force) are the major interactions occurring between the extracts and enzymes. Trp and Asp have previously been identified as common amino acids stabilising the interactions between glucosidase and various ligands, while Tyr was reported for amylase [39–41].

5. Conclusion

This is the first time, to the best of our knowledge, the inhibitory mechanism of *T. catappa* leaf extracts on glucosidase and amylase is being reported, making it an effective agent in managing postprandial hyperglycaemia. These extracts preferably bind to the active site of these enzymes where their various identified compounds synergistically illicit their inhibitory action. From the different GC-MS identified compounds, vitamin E was the most potent ligand that qualified as a potential drug candidate after docking studies. These plants can be leveraged upon as a natural source of not only vitamin E but other antidiabetic compounds for drug formulation. On the other hand, isolation and characterisation of these identified phytocompounds in addition to *in vivo* studies are still required to confirm these findings.

Data Availability

The data used to support the findings of this study are included in the article.

Conflicts of Interest

The authors declare that there are no conflicts of interest regarding the publication of this paper.

Acknowledgments

References

[1] International Diabetes Federation, *IDF Diabetes Atlas*, International Diabetes Federation, Brussels, Belgium, 8th edition, 2017, http://www.diabetesatlas.org.

[2] S. Broadgate, C. Kiire, S. Halford, and V. Chong, "Diabetic macular oedema: under-represented in the genetic analysis of diabetic retinopathy," *Acta Ophthalmologica*, vol. 96, pp. 1–51, 2018.

[3] N. Holman, B. Young, and R. Gadsby, "Current prevalence of type 1 and type 2 diabetes in adults and children in the UK," *Diabetic Medicine*, vol. 32, no. 9, pp. 1119-1120, 2015.

[4] M. A. Akanji, S. O. Olukolu, and M. I. Kazeem, "Leaf extracts of aerva lanata inhibit the activities of type 2 diabetes-related enzymes and possess antioxidant properties," *Oxidative Medicine and Cellular Longevity*, vol. 2018, Article ID 3439048, 7 pages, 2018.

[5] L. M. Katiki, A. C. P. Gomes, A. M. E. Barbieri et al., "Terminalia catappa: chemical composition, in vitro and in vivo effects on Haemonchus contortus," *Veterinary Parasitology*, vol. 246, pp. 118–123, 2017.

[6] U. F. Ezuruike and J. M. Prieto, "The use of plants in the traditional management of diabetes in Nigeria: pharmacological and toxicological considerations," *Journal of Ethnopharmacology*, vol. 155, no. 2, pp. 857–924, 2014.

[7] A. Anand, N. Divya, and P. Kotti, "An updated review of Terminalia catappa," *Pharmacognosy Reviews*, vol. 9, no. 18, pp. 93–98, 2015.

[8] N. Divya and V. A. Anand, "Phytochemical investigation and in vitro anti-diabetic activity of Terminalia catappa leaves," *International Journal of Phytopharmacy*, vol. 4, no. 5, pp. 132–134, 2014.

[9] F. N. Iheagwam, E. I. Nsedu, K. O. Kayode, O. C. Emiloju, O. O. Ogunlana, and S. N. Chinedu, "Bioactive screening and in vitro antioxidant assessment of nauclea latifolia leaf decoction," *AIP Conference Proceedings*, vol. 1954, no. 1, article 030015, 2018.

[10] M. A. Ibrahim and M. S. Islam, "Anti-diabetic effects of the acetone fraction of Senna singueana stem bark in a type 2 diabetes rat model," *Journal of Ethnopharmacology*, vol. 153, no. 2, pp. 392–399, 2014.

[11] S. Sabiu and A. O. T. Ashafa, "Membrane stabilization and kinetics of carbohydrate metabolizing enzymes (α-amylase and α-glucosidase) inhibitory potentials of eucalyptus obliqua L.Her. (Myrtaceae) Blakely ethanolic leaf extract: an in vitro assessment," *South African Journal of Botany*, vol. 105, pp. 264–269, 2016.

[12] B. O. Ajiboye, O. A. Ojo, O. Adeyonu et al., "Inhibitory effect on key enzymes relevant to acute type-2 diabetes and antioxidative activity of ethanolic extract of Artocarpus heterophyllus stem bark," *Journal of Acute Disease*, vol. 5, no. 5, pp. 423–429, 2016.

[13] F. N. Iheagwam, O. O. Ogunlana, O. E. Ogunlana, I. Isewon, and J. Oyelade, "Potential anti-cancer flavonoids isolated from Caesalpinia bonduc young twigs and leaves: molecular docking and in silico studies," *Bioinformatics and Biology Insights*, vol. 13, article 117793221882137, 2019.

[14] A. Waterhouse, M. Bertoni, S. Bienert et al., "SWISS-MODEL: homology modelling of protein structures and complexes," *Nucleic Acids Research*, vol. 46, no. W1, pp. W296–W303, 2018.

[15] N. P. Thao, B. P. T, N. T. Luyen, T. M. Hung, N. H. Dang, and N. T. Dat, "α-Amylase and α-glucosidase inhibitory activities of chemical constituents from Wedelia chinensis (Osbeck.) Merr. leaves," *Journal of Analytical Methods in Chemistry*, vol. 2018, Article ID 2794904, 8 pages, 2018.

[16] K. Sayah, I. Marmouzi, H. Naceiri Mrabti, Y. Cherrah, and M. E. A. Faouzi, "Antioxidant activity and inhibitory potential of Cistus salviifolius (L.) and Cistus monspeliensis (L.) aerial parts extracts against key enzymes linked to hyperglycemia," *BioMed Research International*, vol. 2017, Article ID 2789482, 7 pages, 2017.

[17] Y. Kidane, T. Bokrezion, J. Mebrahtu et al., "In Vitro Inhibition of alpha-amylase and alpha-glucosidase by extracts from Psiadia punctulata and Meriandra bengalensis," *Evidence-Based Complementary and Alternative Medicine*, vol. 2018, Article ID 2164345, 9 pages, 2018.

[18] M. Figueiredo-González, C. Grosso, P. Valentão, and B. P. Andrade, "α-Glucosidase and α-amylase inhibitors from Myrcia spp.: a stronger alternative to acarbose?," *Journal of Pharmaceutical and Biomedical Analysis*, vol. 118, pp. 322–327, 2016.

[19] D. M. Ortíz-Martinez, C. Rivas-Morales, M. A. de la Garza-Ramos, M. J. Verde-Star, M. A. Nuñez-Gonzalez, and C. Leos-Rivas, "Miconia sp. increases mRNA levels of PPAR gamma and inhibits alpha amylase and alpha glucosidase," *Evidence-Based Complementary and Alternative Medicine*, vol. 2016, Article ID 5123519, 6 pages, 2016.

[20] M. I. Kazeem, S. M. Ogungbe, G. M. Saibu, and O. M. Aboyade, "In vitro study on the hypoglycemic potential of Nicotiana tabacum leaf extracts," *Bangladesh Journal of Pharmacology*, vol. 9, no. 2, pp. 140–145, 2014.

[21] M. I. Kazeem, A. M. Mayaki, B. F. Ogungbe, and A. B. Ojekale, "In-vitro studies on Calotropis procera leaf extracts as inhibitors of key enzymes linked to diabetes mellitus," *Iranian Journal of Pharmaceutical Research*, vol. 15, pp. 37–44, 2014.

[22] A. A. Alimi and A. O. T. Ashafa, "An in vitro evaluation of the antioxidant and antidiabetic potential of Sutherlandia Montana E. Phillips & R. A. dyer leaf extracts," *Asian Pacific Journal of Tropical Biomedicine*, vol. 7, no. 9, pp. 765–772, 2017.

[23] Y. Xu, Y. Guo, Y. Gao et al., "Seperation, characterization and inhibition on α-glucosidase, α-amylase and glycation of a polysaccharide from blackcurrant fruits," *LWT*, vol. 93, pp. 16–23, 2018.

[24] P. Wan, X. Yang, B. Cai et al., "Ultrasonic extraction of polysaccharides from Laminaria japonica and their antioxidative and glycosidase inhibitory activities," *Journal of Ocean University of China*, vol. 14, no. 4, pp. 651–662, 2015.

[25] B. Srinivasan, J. V. Rodrigues, S. Tonddast-Navaei, E. Shakhnovich, and J. Skolnick, "Rational design of novel allosteric dihydrofolate reductase inhibitors showing antibacterial effects on drug-resistant Escherichia coli escape variants," *ACS Chemical Biology*, vol. 12, no. 7, pp. 1848–1857, 2018.

[26] B. Srinivasan, J. V. Rodrigues, S. Tonddast-Navaei, E. Shakhnovich, and J. Skolnick, "Correction to rational design of novel allosteric dihydrofolate reductase inhibitors showing antibacterial effects on drug-resistant Escherichia coli escape variants," *ACS Chemical Biology*, vol. 13, no. 5, p. 1407, 2018.

[27] M. C. N. Picot and M. F. Mahomoodally, "Effects of Aphloia theiformis on key enzymes related to diabetes mellitus," *Pharmaceutical Biology*, vol. 55, no. 1, pp. 864–872, 2017.

[28] T. D. Olawole, M. I. Okundigie, S. O. Rotimi, O. Okwumabua, and I. S. Afolabi, "Preadministration of fermented sorghum diet provides protection against hyperglycemia-induced

oxidative stress and suppressed glucose utilization in alloxan-induced diabetic rats," *Frontiers in Nutrition*, vol. 5, 2018.

[29] N. C. Ameachi and C. L. Chijioke, "Evaluation of bioactive compounds in Pseudarenthemum tunicatum leaves using gas chromatography-mass spectrometry," *Scientific Papers Series Management, Economic Engineering in Agriculture and Rural Development*, vol. 18, no. 1, pp. 53–59, 2018.

[30] S. Wahjuni, A. Mayun Laksmiwati, and I. B. P. Manuaba, "Antidiabetic effects of Indonesian bay leaves (Syzygium polyanthum) extracts through decreasing advanced glycation end products and blood glucose level on alloxan-induced hyperglycemic wistar rats," *Asian Journal of Pharmaceutical and Clinical Research*, vol. 11, no. 4, pp. 340–343, 2018.

[31] G. Melappa, R. Channabasava, C. P. Chandrappa, and T. S. Sadananda, "In vitro antidiabetic activity of three fractions of methanol extracts of Loranthus micranthus, identification of phytoconstituents by GC-MS and possible mechanism identified by GEMDOCK method," *Asian Journal of Biomedical and Pharmaceutical Sciences*, vol. 4, no. 34, pp. 34–41, 2014.

[32] M. S. Costamagna, I. C. Zampini, M. R. Alberto et al., "Polyphenols rich fraction from Geoffroea decorticans fruits flour affects key enzymes involved in metabolic syndrome, oxidative stress and inflammatory process," *Food Chemistry*, vol. 190, pp. 392–402, 2016.

[33] E. P. Gutiérrez-Grijalva, M. Antunes-Ricardo, B. A. Acosta-Estrada, J. A. Gutiérrez-Uribe, and J. Basilio Heredia, "Cellular antioxidant activity and in vitro inhibition of α-glucosidase, α-amylase and pancreatic lipase of oregano polyphenols under simulated gastrointestinal digestion," *Food Research International*, vol. 116, pp. 676–686, 2019.

[34] C. C. Udenigwe, M. Gong, and S. Wu, "In silico analysis of the large and small subunits of cereal RuBisCO as precursors of cryptic bioactive peptides," *Process Biochemistry*, vol. 48, no. 11, pp. 1794–1799, 2013.

[35] C. A. Lipinski, "Rule of five in 2015 and beyond: target and ligand structural limitations, ligand chemistry structure and drug discovery project decisions," *Advanced Drug Delivery Reviews*, vol. 101, pp. 34–41, 2016.

[36] I. Azad, M. Nasibullah, T. Khan, F. Hassan, and Y. Akhter, "Exploring the novel heterocyclic derivatives as lead molecules for design and development of potent anticancer agents," *Journal of Molecular Graphics and Modelling*, vol. 81, pp. 211–228, 2018.

[37] V. C. Pérez-Nájera, J. A. Gutiérrez-Uribe, M. Antunes-Ricardo et al., "Smilax aristolochiifolia root extract and its compounds chlorogenic acid and astilbin inhibit the activity of α-amylase and α-glucosidase enzymes," *Evidence-Based Complementary and Alternative Medicine*, vol. 2018, Article ID 6247306, 12 pages, 2018.

[38] F. N. Dewi, C. E. Wood, C. J. Lees et al., "Dietary soy effects on mammary gland development during the pubertal transition in nonhuman primates," *Cancer Prevention Research*, vol. 6, no. 8, pp. 832–842, 2013.

[39] G. Selvaraj, S. Kaliamurthi, and R. Thirugnanasambandam, "Influence of rhizophora apiculata Blume extracts on α-glucosidase: enzyme kinetics and molecular docking studies," *Biocatalysis and Agricultural Biotechnology*, vol. 4, no. 4, pp. 653–660, 2015.

[40] L. Sim, K. Jayakanthan, S. Mohan et al., "New glucosidase inhibitors from an ayurvedic herbal treatment for type 2 diabetes: structures and inhibition of human intestinal maltase-glucoamylase with compounds from Salacia reticulata," *Biochemistry*, vol. 49, no. 3, pp. 443–451, 2010.

[41] O. Sanni, O. L. Erukainure, C. I. Chukwuma, N. A. Koorbanally, C. U. Ibeji, and M. S. Islam, "Azadirachta indica inhibits key enzyme linked to type 2 diabetes in vitro, abates oxidative hepatic injury and enhances muscle glucose uptake ex vivo," *Biomedicine & Pharmacotherapy*, vol. 109, pp. 734–743, 2019.